


# Noninvasive measurement of the vital signs of cancer patients with a dual-path microbend fiber sensor

YING WANG,<sup>1,5</sup> MEIZHENG YOU,<sup>2,5</sup> YANHONG ZHANG,<sup>3</sup> SUMEI WU,<sup>3</sup>  
YI ZHANG,<sup>4</sup> HUICHENG YANG,<sup>1</sup> TING ZHENG,<sup>2</sup> XIAOHUI CHEN,<sup>2</sup>  
ZHIHAO CHEN,<sup>1,6</sup>  XIANHE XIE,<sup>3,7</sup> AND XIAOCHUN ZHENG<sup>2,8</sup>

<sup>1</sup>Fujian Provincial Key Laboratory of Advanced Micro-Nano Photonics Technology and Devices, Quanzhou Normal University, Quanzhou 362000, China

<sup>2</sup>Department of Anesthesiology, Shengli Clinical Medical College of Fujian Medical University, Fujian Provincial Hospital, Fuzhou 350001, China

<sup>3</sup>Department of Oncology, Molecular Oncology Research, The First Affiliated Hospital, Fujian Medical University, Fuzhou 350005, China

<sup>4</sup>School of Informatics, Xiamen University, Xiamen 361005, China

<sup>5</sup>contributed equally

<sup>6</sup>zhihaochen@qztc.edu.cn

<sup>7</sup>xiexianhe@fjmu.edu.cn

<sup>8</sup>zhengxiaochun7766@163.com

**Abstract:** A novel dual-path microbend fiber optic sensor is designed for noninvasive measurement of respiratory rate (RR) and heart rate (HR) for cancer patients. The performance of the microbend fiber sensor is assessed in two groups of cancer patients, cancer patients with pain and without pain, ranging from eighteen to ninety-six years old in a daily observational measurement with the sensor mattress under the mattress of the clinical bed. All the patients received standard clinical monitoring for evaluating the accuracy of our measurement results. The results of our study showed good consistency in the experimental results of RR and HR between the dual-path fiber sensor we proposed and the hospital equipment with average errors of 3.60 beats per minute (bpm) and 1.02 respiration per minute (rpm) in HR and RR measurement in cancer patients with pain and 1.87bpm and 1.27rpm in HR and RR measurement in cancer patients without pain, respectively. In HR monitoring, the single path microbend fiber optic sensor has 8035 minutes of data with a false report rate of 19.09%, while the dual-path microbend fiber optic sensor has 6188 minutes of data with a false report rate of 12.87%. The dual-path sensor has a smaller false report rate compared with the single path sensor due to pre-judgments of data with path 1 and path 2. To our best knowledge, it is the first time to propose and demonstrate a dual-path sensor to reduce the false report rate for HR and RR measurements. The results of the Blend-Altman method showed great agreement between our sensor and hospital standard monitor in HR and RR measurements. The independent sample t-test indicates that the HR of cancer patients may be an effective way to judge whether or not they have cancer pain. Our noninvasive dual-path microbend fiber sensor also showed the advantages of an easy fabrication process, simple structure, and low false report rate.

© 2022 Optica Publishing Group under the terms of the [Optica Open Access Publishing Agreement](#)

## 1. Introduction

Vital signs measurement is an important part of standard medical care to assess the physical conditions and provide proper treatments for cancer pain patients. Heart rate and respiration rate are key elements in the medical department as well as daily home monitoring. Traditional vital signs monitors need direct patient skin contact with the device, which restricts the movement

of patients. Patients with cancer pain, in particular, need a more effective, convenient, and noninvasive way to monitor their vital signs in time.

Among all kinds of new vital signs sensors, like acoustic sensor [1], ECG sensor [2], air mattress sensor [3], electrical sensors [4–7], and optical sensors [8–29], that operate in a noninvasive way are widely studied because they are easy to use and without physical constraint to patients. Among these new sensors, electrical and optical methods are the two typical ways of noninvasively monitoring HR and RR. Electrical methods, including piezo-electric [4] and accelerometry [6,7], are the most popular way to monitor vital signs. However, the electrical sensor systems are vulnerable to the electromagnetic field

The invention of optical fiber sensors provides an alternative way for clinical use because its compact size, stable with electromagnetic interference, and non-toxic. A variety of optical fiber sensors have been studied to monitor vital signs, including photoplethysmography (PPG) fiber sensor [8], polymer optical fiber sensors [9–11], interferometric fiber optics sensors [12–15], fiber Bragg grating sensors [16–19], macro-bend fiber sensor [20], and fiber laser sensor [21], etc. Polymer fiber sensor has lower Young's modulus, larger strain limits, and fracture toughness and good for some applications. Interferometric optical fiber sensors have been widely studied but the demodulation of this method is complex. Wavelength detection for the signal of fiber Bragg grating sensors is too complex and costly for the consumer. The macro-bend sensor has a simple system configuration but the sensitivity may not be adequate for accurate measurement. Microbend fiber sensor has distinct advantages because it has a simple configuration, low cost, good enough sensitivity for HR and RR monitoring. Moreover, the relative intensity variation is applied in microbend fiber sensors for monitoring rather than other sensors' absolute intensity measurement, which makes it more reliable for real world application. Many demonstrations of microbend fiber sensors have been widely studied for vital signs monitoring [22–28]. However, most of their work was applied to a healthy candidates and non-cancer patients. Cancer patients may have more body movements which may disturb RR and HR signals and result in high false report rate. Few works aim at clinical cancer patients particularly.

To meet the clinical demand for cancer patients monitoring, we design and employ a sensitive dual-path microbend fiber sensor for HR and RR monitoring to reduce the rate of a false report. The proposed low-cost sensor is cableless, free of electromagnetic interference, and noninvasive. In this paper, we evaluate the accuracy of the proposed sensor by comparing the data obtained from the clinical standard monitor. Traditional single path monitors have the disadvantage of high false report rate caused by cancer patients' other movements. This is not acceptable for applications. Compared with our previous works [13,27–29], we use a new dual-path sensor in approximately identical conditions to monitor HR and RR. If the difference of the HR or RR between two independent paths is large than 5 bpm or 5 rpm, that set of data will be regarded as wrong data and rounded out. So, the rate of false report will be reduced greatly compared with the single path monitor. In HR monitoring, the single path monitor has 8035 minutes of data with a false report rate of 19.09%, while the dual-path monitor has 6188 minutes of data with a false report rate of 12.87%. This work was cooperated with Fujian Provincial Hospital and the First Affiliated Hospital of Fujian Medical University. One of the aims of this work was to find some key features of the pain within cancer patients and postoperative patients for pain management by measuring vital signs and others. Our proposed sensor can also be used for other groups of patients who need vital signs monitoring. To our best knowledge, it is the first time to propose and demonstrate a dual-path microbend fiber optic sensor to reduce the false report rates. Besides, we consider both the time domain and frequency domain signals to ensure the reliability of the heart rate and respiration rate measurements. Reasonable errors less than 5bpm in HR and 5rpm in RR monitoring are obtained between our dual-path microbend fiber sensor and the standard monitor in clinical environments. The results of the Blend-Altman method show great agreement between our sensor and hospital standard monitor in HR and RR

measurement. The independent sample t-test indicates that the HR of cancer patients may be an effective way to judge whether or not they have cancer pain. Our novel dual-path microbend fiber sensor is promising for long-term healthcare monitoring for cancer patients because of its robustness, simple structure, noninvasive manner, and great agreement with a standard monitor.

## 2. Sensor structure and working principles

Figure 1 depicted the cross-section diagram of a dual-path microbend fiber sensor structure. Two separate layers of graded multimode optical fiber (MMF, YOFC 100/125) are clamped between three layers of hole-mesh to form the dual-path sensor structure. Then the sensor is covered by wallpaper to protect the sensor. According to the microbending optical fiber theory, the body movements and vibrations, like heartbeats and respiration-caused vibrations, can cause fluctuations of the sinusoidal amplitude of the microbend fiber sensor structure.

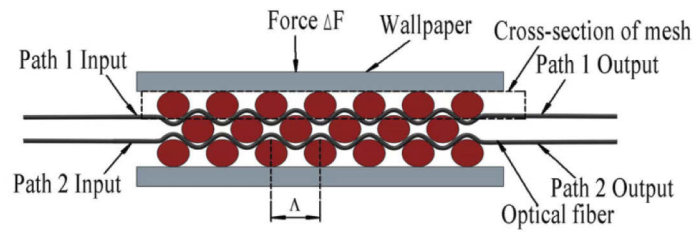


**Fig. 1.** Cross-section pattern of dual-path microbend fiber sensor.

The transmission for the light propagation in the microbend graded multimode fiber is a function of  $\Delta F$  which is the force that the microbending fibers were received and modulated with the body movement or environmental vibrations. By extracting the light intensities, the vital signs could be obtained [27]. The critical mechanical pitch, known as  $\Lambda$ , is given by

$$\Lambda = \frac{2\pi an}{NA} \quad (1)$$

where  $a$  is the core radius of the fiber,  $n$  is the refractive index (RI) of the core and  $NA$  is the numerical aperture in the fiber. If the equation of (1) is met, the maximum sensitivity of the sensor may be achieved.

To get the accurate value of RR and HR, time domain and frequency domain methods were applied, respectively. For RR measurement, we count the envelope of the time domain signal in path 1 and path 2 to get  $RR_1$  and  $RR_2$ . If  $|RR_1 - RR_2| \geq 5\text{rpm}$ , that set of data will be regarded as false data. If  $|RR_1 - RR_2| < 5\text{rpm}$ , the final RR is obtained by

$$RR = (RR_1 + RR_2)/2 \quad (2)$$

For HR measurement, we first use time domain method to get a HR, then used frequency domain method to verify and correct the final result by using multi harmonic frequency peaks as follows.

In the frequency domain method, the N-order harmonic wave of HR signal in path 1 is defined as  $f_{1N}$ . Then the HR in path 1 using different harmonic waves is calculated by

$$\begin{aligned} HR_{11} &= f_{11} * 60 \\ HR_{12} &= (f_{12}/2) * 60 \\ &\dots\dots\dots \\ HR_{1N} &= (f_{1N}/N) * 60 \end{aligned} \quad (3)$$

So, the HR in path 1 is obtained by

$$HR_1 = (HR_{11} + HR_{11} + \dots + HR_{1N})/N \quad (4)$$

Similarly, the HR in path 2 can be calculated by

$$HR_2 = (HR_{21} + HR_{21} + \dots + HR_{2N})/N \quad (5)$$

If  $|HR_1 - HR_2| \geq 5\text{bpm}$ , that set of data will be regarded as false data. If  $|HR_1 - HR_2| < 5\text{bpm}$ , the final HR is obtained by

$$HR = (HR_1 + HR_2)/2 \quad (6)$$

To illustrate the unique advantage of our proposed dual-path sensor for reducing the rate of a false report, Fig. 2 gives a typical result of HR measurement. For single path case, path 2 is regarded as a single path result and will be reported directly without any judgment. If  $|HR_{\text{monitor}} - HR_{\text{path 2}}| \geq 5\text{bpm}$ , that set of data may be wrong data and may lead high false report rate. In our dual-path case, we add one more step before data reporting, that is, evaluating if  $|HR_{\text{path 1}} - HR_{\text{path 2}}| < 5\text{bpm}$ . If  $|HR_{\text{path 1}} - HR_{\text{path 2}}| \geq 5\text{bpm}$ , that set of data will not be reported. The false report rate can be reduced greatly by employing this pre-processing method.

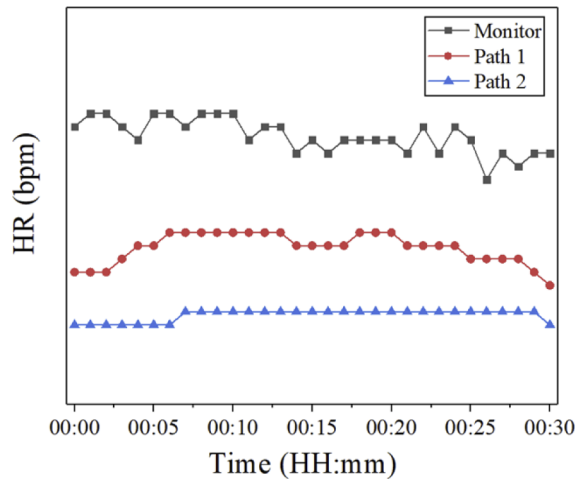


**Fig. 2.** Examples of HR data.

### 3. Experimental result and discussion

We analyze clinical experiments of cancer patients and postoperative patients carried out in two hospitals from 2020 to 2021. In order to illustrate the unique advantage of the ability of our dual-path microbend fiber optic sensor to reduce the false-report rate of, two kinds of microbend fiber optic sensor, the single path and dual-path sensors, are applied in postoperative and cancer patients, respectively. Approval from the Ethics Committee of Fujian Provincial Hospital (K2020-03-021), Ethics Committee of the First Affiliated Hospital of Fujian Medical University (MRCTA, ECFAH of FMU [2020] 165), and full patients' consent was obtained. In the First Affiliated Hospital of Fujian Medical University, one hundred and two cancer patients with pain and one hundred and nine cancer patients without pain were recruited in the study. As for comparison, 223 postoperative patients were recruited in Fujian Provincial Hospital.

### 3.1. Setup

The schematic configuration of microbend fiber sensor system is shown in Fig. 3(a) and the dual-path configuration of the fiber sensing system is depicted in Fig. 3(b). The monitoring system has a dual-path sensor, a homemade transceiver, a hospital standard ECG monitor, and a computer. The optical transceiver consists of two pairs of light sources and detectors, a microprocessor, and a circuit for noise reduction. The light sources are connected to two layers of microbend fiber with a thickness of  $\sim 2$  mm, respectively. Then, the fibers are connected to two detectors in the transceiver to form two identical sensor paths. Path 1 of our sensor consists of light sources 1, microbend mesh, detectors 1, MCU and computer. Path 2 of our sensor consists of light sources 2, microbend mesh, detectors 2, MCU and computer. The transceiver receives fluctuate signals and transmits them to the computer which is sampled at 50 Hertz (Hz) via Bluetooth. Moreover, the commercial ECG monitor is used to provide the reference value of HR and RR, to judge the accuracy of the proposed sensor. Figure 4 shows the prototype of the sensor mattress we designed for the clinical trial use. It should be noticed that all patients were required to lie in the clinical bed with the sensing mattress under them.

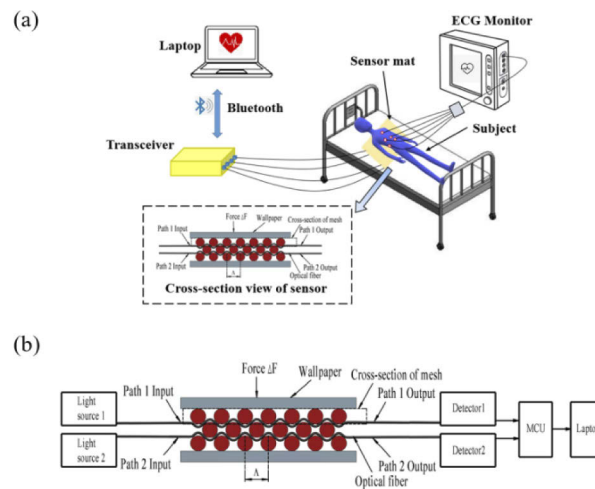


**Fig. 3.** The schematic configuration of microbend fiber sensor system.

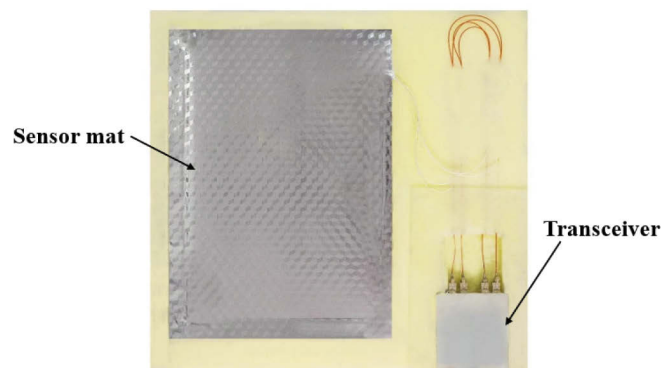


**Fig. 4.** The prototype of the sensor mattress.

### 3.2. Measurement

To begin with, we analyzed the method of HR and RR measurement. In general, the HR of adults is about 45-100bpm (0.75Hz~1.66Hz), and the RR is 6~30rpm (0.1~0.5Hz) roughly.

Here, we take patient #5 as an example to figure out how we calculate the RR and HR. The HR and RR are obtained by counting the envelopes and peaks of the time domain signals roughly. Figure 5(a) and (b) depict the raw data of a cancer pain patient (patient #5) detected by the proposed dual-path sensor in 16 seconds, respectively. The signal is a mixture of HR and RR signals, and the signals detected by path 1 and path 2 have a similar trend. There are four envelopes within 16 seconds in Fig. 5(a), we can roughly count the RR as  $60 * (4/16) = 15\text{rpm}$  of patient #5 in path 1. As for HR, the 4-order Butterworth filtering is employed in the raw data. The HR signal after signal processing is seen clearly in Fig. 5(c) and (d), the HR of patient #5 is counted it as  $60 * (19/16) = 71.25\text{bpm}$  in path 1. The raw data of path 2 was processed by the same procedure, and RR and HR are 15rpm and 71.25bpm. To ensure the accuracy of our measurement, the frequency-domain method is also applied.

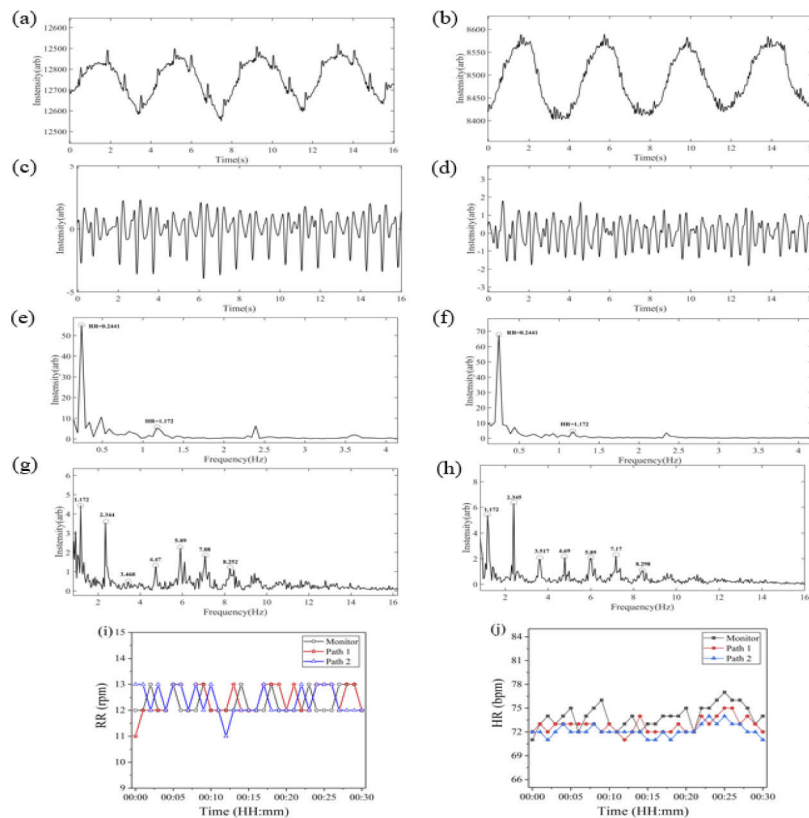


**Fig. 5.** (a) raw data of patient #5 detected in path 1; (b) raw data of patient #5 detected in path 2; (c) HR signal of patient #5 in path 1 after filtering; (d) HR signal of patient #5 in path 2 after filtering; (e) frequency-domain RR signal of patient #5 in path 1; (f) frequency-domain RR signal of patient #5 in path 2; (g) frequency-domain HR signal of patient #5 in path 1; (h) frequency-domain HR signal of patient #5 in path 2; (i) 30-min detected RR signal of patient #5; (j) 30-min detected HR signal of patient #5.

Then, the HR and RR are calculated accurately in the frequency domain. Figure 5(e) and (f) give the Fast Fourier Transformation (FFT) spectra of the raw data of paths 1 and 2 in the 0-4Hz range, respectively. The RR is counted as 15rpm (0.25Hz) in the time-domain, while the



frequency-domain has a peak of 0.2441Hz in Fig. 5(e), the peak of the frequency signal of RR is easily identified, and calculated as  $60 * 0.2441 = 14.65$  rpm in path 1. As for path 2, the RR is calculated as  $60 * 0.2441 = 14.65$  rpm in Fig. 5(f). The FFT spectra in the 0-20Hz range is shown in Fig. 5 (g) and (h). The frequency-domain signal also has a main peak of 1.172Hz, and the HR is calculated as  $60 * 1.172 = 70.32$ bpm in Fig. 5(g). Figure 5(h) shows the FFT spectrum of raw data in path 2, the main peak of 1.172Hz is identified and the HR is  $60 * 1.172 = 70.32$ bpm. The results show a great agreement in the time domain and frequency-domain with 0.35rpm and 0.93bpm differences in RR and HR measurements, respectively. We use the time domain processing method for RR measurement in the final experimental results because the quality of the RR signals was very good as such the frequency domain method were not needed. However, the heart beat signals were noisy, we need both time domain and frequency domain method to obtain final HR. In this case, we first used time domain method to get a HR, then used frequency domain method to verify and correct the final results by using multi harmonic frequency peaks in our final experimental results.

We record the RR and HR in 30 minutes of each patient with 1 value per second using our dual-path microbend sensor and with 1value per minute using the reference monitor. The results of sensor-detected RR and standard ECG of patient #5 in 30 minutes are shown in Fig. 5(i). Figure 5(j) shows the results of sensor-detected HR and standard ECG of patient #5 in 30 minutes.

### 3.3. RR and HR analysis of cancer pain patients

As we defined before, two groups of cancer patients, with/without cancer pain, are studied in this paper, and this part will show the results of cancer pain patients. Figure 6 illustrates the RR monitoring results of one typical example monitoring by our microbend fiber sensor and commercial monitor in 30 minutes. Figure 7 illustrates the HR monitoring result of one typical example of monitoring by the microbend fiber sensor and commercial monitor in 30 minutes.

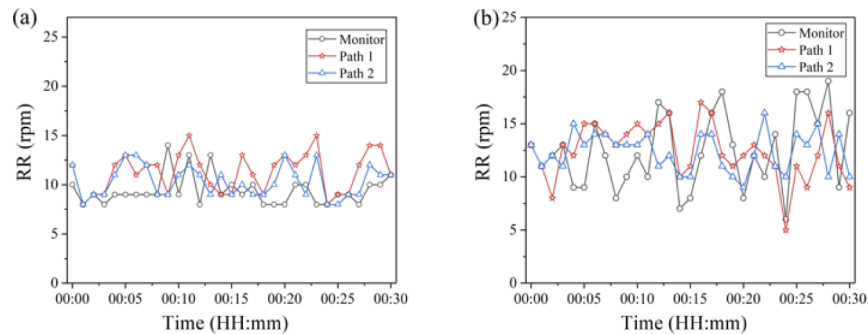


**Fig. 6.** Typical RR of cancer patients with pain: (a) patient #16, (b) patient #21.

According to the American National Standards Institute definition, a readout error of no greater than the input rate or  $\pm 5$  beats per minute is acceptable [7,30]. It is important to perform the consistency experiments between the result of dual-path sensor and commercial monitor. For that target, the Bland-Altman method [31] is applied. The mean difference between the dual-path sensor and the standard monitor, and the 95% confidential interval (CI) ( $\pm 1.96SD$ ) is determined for both RR and HR measurements. As shown in Fig. 8(a) and (b), the consistency of RR and HR measurement is displayed. There are 107 and 112 sets of data in RR and HR, respectively. We use  $x_1$  to stand for the mean of RR or HR monitored by the dual path sensor, and use  $x_2$  to stands for the RR or HR results monitored by standard ECG.  $x_1 - x_2$  denotes the RR or HR mean the difference between dual-path sensor and standard monitor.  $(x_1 + x_2)/2$  stands for the average of RR or HR measured by dual-path sensor and standard monitor. The results showed the mean

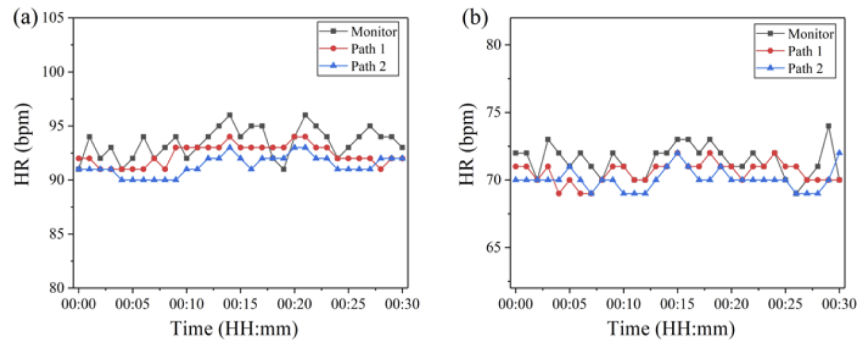


**Fig. 7.** Typical HR of cancer patient with pain: (a) patient #16, (b) patient #21.

HR difference is 1.01 bpm and the mean RR difference is 2.30 rpm. The SDs of mean difference of RR and HR in patients with pain are 2.69rpm and 4.48bpm, respectively. So, the CI of difference in RR is  $[-4.37; 6.39]$ , and the CI of mean difference in HR is  $[-6.66; 12.26]$ . 97.20% (104/107) of the RR differences and 95.54% (107/112) of the HR differences are distributed within  $\pm 1.96$  SD range, which is redeemed good consistency with the Bland-Altman method.

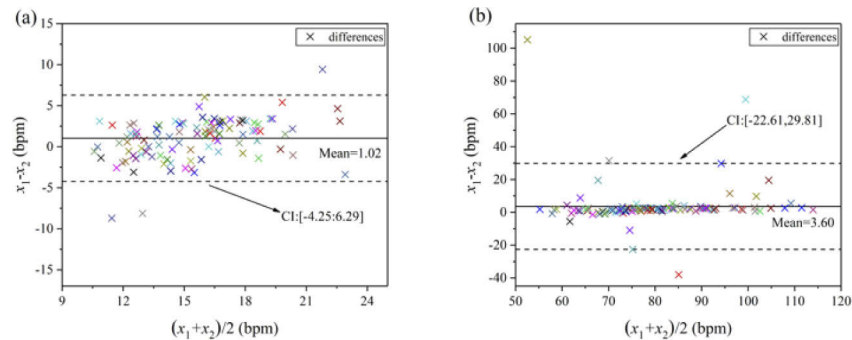


**Fig. 8.** (a) Mean differences and CI of RR with cancer pain patients; (b) mean differences and CI of HR with cancer pain patients.

### 3.4. HR and RR analysis of cancer patients without pain

As for HR and RR measurements of cancer patients without pain, we use the same procedure for cancer patients with pain. Figure 9 illustrates the RR measurement results of several typical examples of monitoring by the microbend fiber sensor and commercial monitor in 30 minutes. Figure 10 illustrates the HR measurement results of several typical examples monitored by the microbend fiber sensor and commercial monitor in 30 minutes. The results show great agreement between our sensor and commercial monitor.

As shown in Fig. 11(a) and (b), the consistency of RR and HR measurement is displayed. There are 98 and 106 sets of data in RR and HR, respectively. As a result, the mean RR difference is 1.43 rpm and the mean HR difference is 1.87 bpm. The SDs of mean difference of RR and HR in patients with pain are 2.32rpm and 3.68bpm, respectively. So, the CI of mean difference in RR is  $[-3.23; 6.09]$ , and the CI of mean difference in HR is  $[-5.49; 9.23]$ . 95.28% (101/106) of the RR differences and 94.90% (93/98) of the HR differences are distributed within  $\pm 1.96$  SD range, which is redeemed good consistency with the Bland-Altman method.



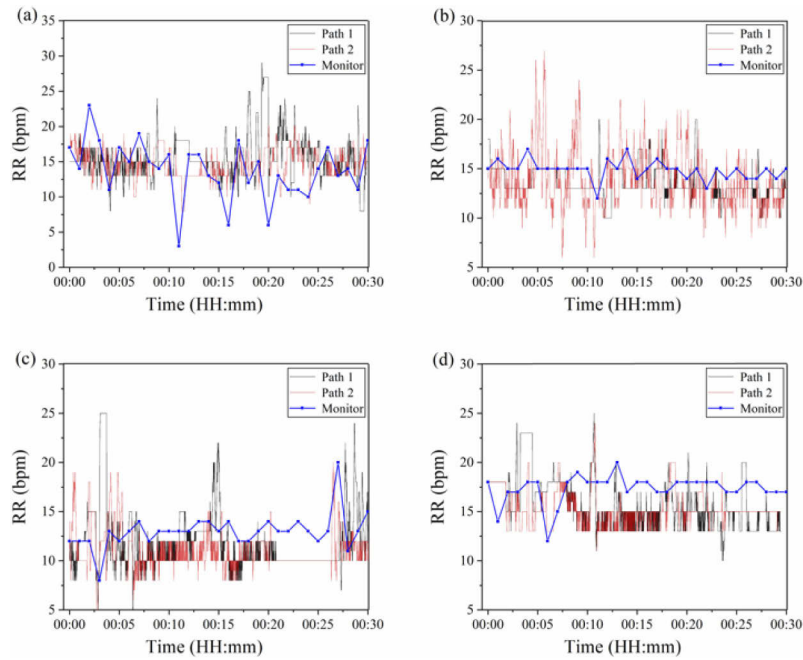


**Fig. 9.** Typical HR signals of cancer patients without pain: (a) patients #123, (b) patients #136, (c) patients #142, (d) patients #190.

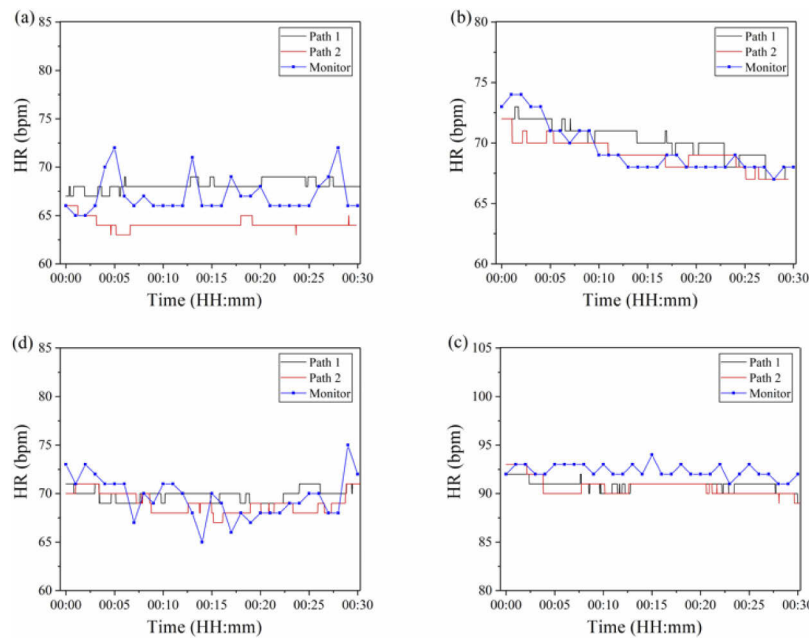


**Fig. 10.** Typical HR signals of cancer patients with pain: (a) patients #128, (b) patients #161, (c) patients #182, (d) patients #197.

To summary, the mean differences between our sensor and standard monitor of cancer patients with/without pain are listed in Table 1. 112 sets of effective data of cancer pain people are

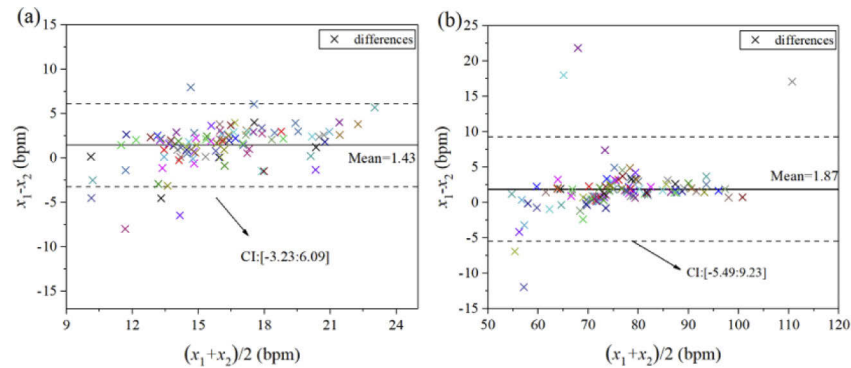


**Fig. 11.** (a) Mean differences and CI of RR with cancer patients without pain; (a) mean differences and CI of HR with cancer patients without pain.

calculated in HR measurement and 107 sets of effective data for RR calculating. 106 sets of effective data of cancer patients without pain is calculated in HR measurement and 98 sets of effective data for RR calculating. The mean differences of RR measurement of cancer patients with/without pain are 1.01rpm and 1.27rpm, respectively, while the mean differences of HR measurement of cancer patients with/without pain are 2.69bpm and 1.87bpm, respectively. All these results are acceptable according to [7,29] with less than 5bpm or 5rpm differences.

**Table 1. Mean difference between our dual-path sensor and standard monitor.**

Mean difference	RR(Rpm)	HR (bpm)
With pain	1.01	2.69
Without pain	1.43	1.87

### 3.5. Measurements using single path sensor

We also carry out RR and HR measurements using a single path microbend sensor for comparison in Table 2. 217 sets of data of cancer pain people are calculated in HR measurement and 206 sets of data for RR calculating. The mean differences of HR and RR measurement are 2.98bpm and 5.38rpm, respectively. Dual-path sensor has small mean difference both in HR and RR measurement compared with single path sensor.

**Table 2. Mean difference between our single path sensor and standard monitor.**

	HR(bpm)	RR (rpm)
Mean difference	2.98	5.38

### 3.6. Discussion

The false report rate of HR with a single path and dual-path monitors is given in Table 3. As mentioned before, 102 cancer patients with pain and 109 cancer patients without pain are recruited in the study in one hospital. As for comparison, 223 postoperative patients are recruited in another hospital. Every patient will be tested in a period of 30 to 60 minutes with data record of 1 value per minute. In particular, if the record data from hospital equipment is equal to zero in RR (larger than 2-minute data) or has no data in the documentary file, that set of data will be

rounded out. Finally, the single path sensor has 8035 minutes of data, which is extracted from the data of 223 postoperative patients. The single path sensor has a false report rate of 19.09%, while the dual-path monitor has 6188 minutes of data with a false report rate of 12.87%. As we can find out through the result, dual-path monitor has a small false report rate compared with single path monitor because of the pre-judge process. If the difference between two independent paths is large than 5 bpm in dual-path monitor, that set of data will be regarded as wrong data and rounded out. So, the rate of false report is reduced greatly compared with the single path monitor. To our best knowledge, it is the first time to propose and demonstrate a dual-path monitor to reduce the false report rate in the clinical environment.

**Table 3. False report rates of single path and dual-path sensor of HR.**

Type	Data number	False report number	False report rate (%)
Single path	8035	1506	19.09
Dual-path	6188	795	12.87

Table 4 shows the independent sample t-test of the HR and RR results. According to Table 4, the mean of RR and HR and SD of RR and HR in cancer patients with or without pain are obtained, and the correlation factor *P* between cancer patients with pain and without pain in HR and RR measurements using our noninvasive dual-path microbend fiber sensor is evaluated. From Table 4, there is a significant difference between cancer patients with or without pain in HR with  $P < 0.05$ , and there is no significant difference between cancer patients with or without pain in RR with  $P > 0.05$ . Therefore, the sensor may provide a noninvasive measurement method for judging whether a cancer patient has pain or not through HR measurement.

**Table 4. Mean and standard deviation of HR and RR, and independent sample t-test results.**

	HR(bpm)	RR (rpm)
With pain	78.15±14.65	14.98±3.10
Without pain	74.88±10.15	15.35±2.83
<i>P</i>	0.019	0.497

Very few publications with other similar solutions so far are found to address this false report issue. Many solutions are based on software solution in a single sensor [32–34]. The software solutions are suffered and limited by the signal quality in the real-world application. As for multiple sensor solution [33], it uses Cepstrum analysis and sensor fusion and has the problem that every single sensor suffers different noisy environments and cannot guarantee the uniformity of variables. Compared with the multiple FBG sensor solution, our work has two independent paths integrated in the same sensor structure that suffers the same environmental variables and thus good signal quality is easily judged. Therefore, our sensor solution will have better performances in the real-world applications.

#### 4. Conclusion

We have designed a novel dual-path microbend fiber optic sensor to measure HR and RR for cancer patients in clinical monitoring cases. Here, we separate the cancer patients into two groups, cancer pain patients and non-cancer pain patients. The spectra of the microbend fiber sensor fluctuate with the patients' body movements, like RR, HR and other noise signals. The clinical standard monitor is applied for comparison, and the experimental results show great agreement between the commercial monitor and the proposed sensor with average errors of 3.60bpm and 1.02rpm of cancer patients with pain in HR and RR measurement, respectively. And the average

errors of 1.86bpm and 1.27rpm of cancer patients without pain in HR and RR measurement are obtained, respectively. We also applied single path sensor with postoperative patients for comparison. In HR monitoring, the single path sensor has 8035 minutes of data with a false report rate of 19.09%, while the dual-path sensor has 6188 minutes of data with a false report rate of 12.87%. Dual-path sensor has a smaller false report rate compared with single path sensor due to pre-judgments of data with our dual sensor paths. To our best knowledge, it is the first time to propose and demonstrate a dual-path sensor to reduce the false report rate. The results of the Blend-Altman method show great agreement between our sensor and hospital standard monitor in HR and RR measuring. The independent sample t-test indicates that the HR of cancer patients may be a biomarker to judge whether or not they have cancer pain. Our noninvasive dual-path microbend fiber sensor also has advantages of simple structure, easy fabrication, very low power consumption and low cost. The proposed dual-path noninvasive microbend fiber sensor is a good candidate for application fields where traditional adhesive electrode method is not available, such as high electromagnetic field areas, and where noninvasive methods are needed. We expect this new sensor will be used widely at home due to very low cost and high performance.

**Funding.** the Innovation of Science and Technology (2019Y9023, 2019Y9028); the Fund of University-Industry Research Project from Department of Science and Technology (2021H6013); Medical Innovation Project of Fujian Province (2020CXB002); Fund of “Harbour Project” of Quanzhou (2017ZT013).

**Acknowledgments.** This work was supported by the Fund of University-Industry Research Project from Department of Science and Technology, Fujian Province (Grant No. 2021H6013); the Joint Funds for the Innovation of Science and Technology, Fujian Province (Grant Nos. 2019Y9028 and 2019Y9023); the Medical Innovation Project of Fujian Province (Grant No. 2020CXB002); the Fund of “Harbour Project” of Quanzhou (Grant No. 2017ZT013).

**Disclosures.** The authors declare no conflicts of interest.

**Data availability.** Data underlying the results presented in this paper are not publicly available at this time but may be obtained from the authors upon reasonable request.

## References

1. M. V. Scanlon, “Acoustically monitor physiology during sleep and activity,” *Proceedings of the First Joint BMES/EMBS Conference, 1999 IEEE Engineering in Medicine and Biology 21st Annual Conference and the 1999 Annual Fall Meeting of the Biomedical Engineering Society*, volume 2 (1999), p. 787.
2. P. de Chazal, C. Heneghan, E. Sheridan, R. Reilly, P. Nolan, and M. O’Malley, “Automated processing of the single-lead electrocardiogram for the detection of obstructive sleep apnea,” *IEEE Trans. Biomed. Eng.* **50**(6), 686–696 (2003).
3. Y. Chee, J. Han, J. Youn, and K. Park, “Air mattress sensor system with balancing tube for unconstrained measurement of respiration and heartbeat movements,” *Physiol. Meas.* **26**(4), 413–422 (2005).
4. G. Roopa, K. Rajanna, and M. M. Nayak, “Non-invasive human breath sensor,” *Proc. IEEE Sensors* **2011**, 1788–1791 (2011).
5. J. Liu, Y. Chen, Y. Wang, X. Chen, J. Cheng, and J. Yang, “Monitoring vital signs and postures during sleep using WiFi signals,” *IEEE Internet of Things Journal* **5**(3), 2071–2084 (2018).
6. Y. Zhang and W. S. Kim, “Highly sensitive flexible printed accelerometer system for monitoring vital signs,” *Soft Robot.* **1**(2), 132–135 (2014).
7. F. Jacobs, J. Scheerhoorn, E. Mestrom, J. vander Stam, R. A. Bouwman, and S. Nienhuijs, “Reliability of heart rate and respiration rate measurements with a wireless accelerometer in postbariatric recovery,” *PLoS ONE* **16**(4), e0247903 (2021).
8. Lindberg, H. Ugnell, and P. Oberg, “Monitoring of respiratory and heart rates using a fibre-optic sensor,” *Med. Biol. Eng. Comput.* **30**(5), 533–537 (1992).
9. A. G. Leal-Junior, C. R. Díaz, C. Leitão, M. J. Pontes, C. Marques, and A. Frizera, “Polymer optical fiber-based sensor for simultaneous measurement of breath and heart rate under dynamic movements,” *Opt. Laser Technol.* **109**, 429–436 (2019).
10. A. Leal-Junior, L. Avellar, A. Frizera, P. Antunes, C. Marques, and C. Leitão, “Polymer optical fibers for mechanical wave monitoring,” *Opt. Lett.* **45**(18), 5057–5060 (2020).
11. P. Han, L. Li, H. Zhang, L. Guan, C. Marques, S. Savović, and X. Li, “Low-cost plastic optical fiber sensor embedded in mattress for sleep performance monitoring,” *Opt. Fiber Technol.* **64**, 102541 (2021).
12. S. Wang, X. Ni, L. Li, J. Wang, Q. Liu, Z. Yan, L. Zhang, and Q. Sun, “Noninvasive monitoring of vital signs based on highly sensitive fiber optic mattress,” *IEEE Sensors J.* **20**(11), 6182–6190 (2020).
13. F. C. Favero, V. Pruneri, and J. Villatoro, “Microstructured optical fiber interferometric breathing sensor,” *J. Biomed. Opt.* **17**(3), 037006 (2012).

14. W. Chen, Y. Zhang, H. Yang, Y. Qiu, and C. Yu, "Non-invasive measurement of vital signs based on seven-core fiber interferometer," *IEEE Sens. J.* **21**(9), 10703–10710 (2021).
15. W. Xu, Y. Shen, C. Yu, B. Dong, W. Zhao, and Y. Wang, "Long modal interference in multimode fiber and its application in vital signs monitoring," *Opt. Commun.* **474**, 126100 (2020).
16. A. Silva, J. Carmo, P. Mendes, and J. Correia, "Simultaneous cardiac and respiratory frequency measurement based on a single fiber Bragg grating sensor," *Meas. Sci. Technol.* **22**(7), 075801 (2011).
17. L. Dziuda, F. W. Skibniewski, M. Krej, and P. M. Baran, "Fiber Bragg grating-based sensor for monitoring respiration and heart activity during magnetic resonance imaging examinations," *J. Biomed. Opt.* **18**(5), 057006 (2013).
18. M. Fajkus, J. Nedoma, R. Martinek, V. Vasinek, H. Nazeran, and P. Siska, "A non-invasive multichannel hybrid fiber-optic sensor system for vital sign monitoring," *Sensors* **17**(12), 111 (2017).
19. T. D. Allsop, T. Earthrowl-Gould, D. J. Webb, and I. Bennion, "Embedded progressive-three-layered fiber long-period gratings for respiratory monitoring," *J. Biomed. Opt.* **8**(3), 552–559 (2003).
20. A. Grillet, D. Kinet, J. Witt, M. Schukar, K. Krebber, F. Pirotte, and A. Depré, "Optical fiber sensors embedded into medical textiles for healthcare monitoring," *IEEE Sensors J.* **8**(7), 1215–1222 (2008).
21. J. Wo, H. Wang, Q. Sun, P. P. Shum, and D. Liu, "Noninvasive respiration movement sensor based on distributed Bragg reflector fiber laser with beat frequency interrogation," *J. Biomed. Opt.* **19**(1), 017003 (2014).
22. H.-F. Hu, S.-J. Sun, R.-Q. Lv, and Y. Zhao, "Design and experiment of an optical fiber micro bend sensor for respiration monitoring," *Sens. Actuators A: Phys.* **251**, 126–133 (2016).
23. D. Lau, Z. Chen, J. T. Teo, S. H. Ng, H. Rumpel, Y. Lian, and P. L. Kei, "Intensity-modulated microbend fiber optic sensor for respiratory monitoring and gating during MRI," *IEEE Trans. Biomed. Eng.* **60**(9), 2655–2662 (2013).
24. Z. Chen, D. Lau, J. T. Teo, S. H. Ng, X. Yang, and P. L. Kei, "Simultaneous measurement of breathing rate and heart rate using a microbend multimode fiber optic sensor," *J. Biomed. Opt.* **19**(5), 057001 (2014).
25. Z. Chen, J. T. Teo, S. H. Ng, X. Yang, B. Zhou, Y. Zhang, and M. Thong, "Monitoring respiration and cardiac activity during sleep using microbend fiber sensor: a clinical study and new algorithm," in *Proc. 36th Annu. Int. Conf. IEEE Eng. Med. Biol. Soc.* (2014), pp. 5377–5380.
26. X. Yang, Z. Chen, C. S. M. Elvin, L. H. Y. Janice, S. H. Ng, J. T. Teo, and R. Wu, "Textile fiber optic microbend sensor used for heartbeat and respiration monitoring," *IEEE Sensors J.* **15**(2), 757–761 (2015).
27. Y. Zhang, Z. Chen, W. Chen, and H. Li, "Unobtrusive and continuous BCG-based human identification using a microbend fiber sensor," *IEEE Access* **7**, 72518–72527 (2019).
28. Y. Zhang, Z. Chen, and H. I. Hee, "Noninvasive measurement of heart rate and respiratory rate for perioperative infants," *J. Lightwave Technol.* **37**(11), 2807–2814 (2019).
29. Q. Wang, Y. Zhang, G. Chen, Z. Chen, and H. I. Hee, "Assessment of heart rate and respiratory rate for perioperative infants based on elc model," *IEEE Sens. J.* **21**(12), 13685–13694 (2021).
30. ANSI/AAMI. Cardiac Monitors, Heart Rate Meters, and Alarms. Arlington: American National Standards Institute, Inc; (2002).
31. M. Lu, W. Zhong, L. Yu-Xiu, H. Miao, Y. Li, and M. Ji, "Sample size for assessing agreement between two methods of measurement by Bland-Altman method," *Int. J. Biostat.* **12**(2), 2 (2016).
32. Y. Zhu, J. Maniyeri, V. F. S. Fook, and H. Zhang, "Estimating respiratory rate from FBG optical sensors by using signal quality measurement," in *2015 37th Annual International Conference of the IEEE Engineering in Medicine and Biology Society (EMBC)* (2015), pp. 853–856.
33. Y. Zhu, V. F. S. Fook, E. H. Jianzhong, J. Maniyeri, C. Guan, H. Zhang, and Biswas, "Heart rate estimation from FBG sensors using cepstrum analysis and sensor fusion," in *2014 36th Annual International Conference of the IEEE Engineering in Medicine and Biology Society* (2014), pp. 5365–5368.
34. V. F. S. Fook, M. Jayachandran, E. P. Jiliang, Z. Yongwei, and E. H. Jianzhong, "Fiber Bragg grating-based monitoring and alert system for care of residents in nursing homes," in *2018 IEEE 4th World Forum on Internet of Things (WF-IoT)* (2018), pp. 195–200.